CFD ANALYSIS OF THE FLOW AROUND A COMPUTER SIMULATED PERSON IN A DISPLACEMENT VENTILATED ROOM

Chris N. Sideroff and Thong Q. Dang
STAR Center in Environmental Quality Systems
Syracuse University, Syracuse, New York, USA

ABSTRACT

This paper gives a summary of a detailed Computational Fluid Dynamics (CFD) study of the flow around a Computer Simulated Person (CSP) in an otherwise empty displacement ventilated room. This study identifies the requirements of several computational aspects such as convergence criteria and grid resolution that are needed for accurate CFD simulations of the personal micro-environment. Two important flow structures, one in the thermal plume and another, the recirculating flow in the room, made it difficult to determine convergence; hence care must taken when monitoring convergence. A grid study highlighted the influence of grid resolution on the recirculating flow path while showing a weaker influence on the thermal plume. Two RANS turbulence models, the standard k-ε with an advanced wall treatment and the v^2-f, predicted different behavior in both flow structures; however without experimental data the results could not be validated.

1. INTRODUCTION

CFD is one of many tools used by researchers to study indoor air quality and thermal comfort of a building occupant's micro-environment. Due to the flexibility and potentially lower costs, CFD allows detailed studies of the Personal Micro-Environment (PME) that supplement experiments. However, its use for PME flows requires thorough verification and validation. The low-speed flows, strong thermal effects, species and particulate transport typical of the personal micro-environment, each with their own difficulties, together make verification and validation a daunting task.

Nielsen, Murakami, Kato, Topp and Yang have combined efforts and provided two benchmark tests for evaluating CFD in the personal micro-environment (Nielsen et al. 2003). Their collaboration proposes two typical building environment scenarios of the mixing and displacement ventilation type with a centrally situated CSP. Only the displacement ventilation setup was examined here. The objective of this study was to illustrate the difficulties encountered when trying to predict the detailed flows of the personal micro-environment with CFD.

2. DISPLACEMENT VENTILATION SETUP

A detailed description of the displacement ventilation geometry, boundary conditions and measurement locations is provided in Nielsen et al. (2003). This paper includes only the displacement ventilation results as the mixing ventilation has been presented in earlier work. Figure 1 illustrates the benchmark displacement ventilation setup used for the simulations including two points (A and B) used to monitor convergence. For reference, the velocity and temperature at the inlet were 0.2 *m/s* and 22° C, respectively, a convective heat load of 38 *W* on the CSP and adiabatic walls, floor and ceiling. All other boundary conditions are outlined in Nielsen et al. (2003). Six measurement locations are included to allow consistent comparison between researchers but no experimental or other computational data were

available at the time for validation. The standing CSP geometry was obtained from Kato's research group at the University of Tokyo.

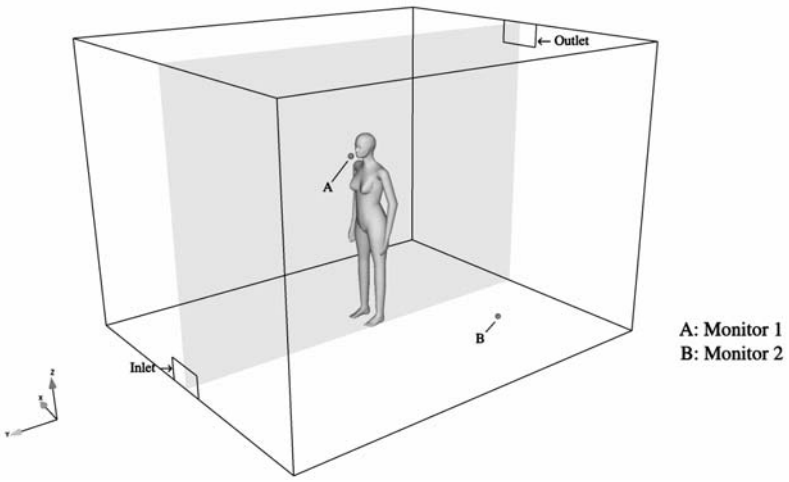

Figure 1. *Displacement Ventilation Room Configuration*

3. COMPUTATIONAL ASPECTS

All simulations were performed with FLUENT (v. 6.2) and the succeeding paragraph outlines the models used. The numerical convective scheme used for all transport equations was a 2nd order accurate upwind scheme. Pressure and velocity were coupled with the SIMPLEC algorithm. Pressure interpolation was achieved with a 2nd order accurate scheme similar to the 2nd order upwind convective scheme. A Beowulf cluster with 64 1.6 GHz processors (x86-64 architecture) and 64 Gbytes of total system memory made this type of analysis possible. Sixteen processors were typically used, which took anywhere from 96 to 144 hours depending on the grid resolution and turbulence model.

4. CONVERGENCE

Displacement ventilation is described as the venting of cool air into the bottom of a room where internal heat sources cause the cooler air to rise, carrying with it any contaminants picked up along its path. It was found during the convergence of the solutions that two distinct flow structures developed. The thermal plume, which was expected, and another not so obvious flow structure was a recirculating flow around the room generated by the inlet vent. The momentum of the inlet vent created a low-speed jet that progressed along the floor, and instead of rising upon hitting the warm feet of the CSP, it proceeded along to the back wall. In fact, the flow circulated several times, three or more times in some instances, before being entrained in the thermal plume. It is critical to accurately predict this flow pattern since pollutant exposure depends on the path of the flow, e.g. particulate matter (PM) transport. The development of these two important flow structures made the judgment of convergence non-trivial.

FLUENT uses averaged residuals to monitor convergence of transport equations. The continuity (and other equations) residual typically dropped 4-5 orders of magnitude (see Fig. 2(a)) and leveled out after about 9000 iterations, possibly indicating convergence. To confirm convergence, a point in the thermal plume (point A in Fig. 1) and another point in recirculating flow (point B in Fig. 1) were monitored during the iteration process. Figure 2(b) shows the very different convergence behaviors at the monitor points during the iteration process. The velocity in the thermal plume (point A) appeared to stop changing at about 9000

iterations and if only this point had been monitored, one would have incorrectly assumed the solution was converged. At 10,000 iterations the velocity increased again and required a further 16,000 iterations to become steady. The velocity in the recirculating flow (point B) did not reach a steady-state until about 26,000 iterations. Because two distinct flow structures developed care must be taken when evaluating convergence - averaged residuals were not a good indicator of convergence.

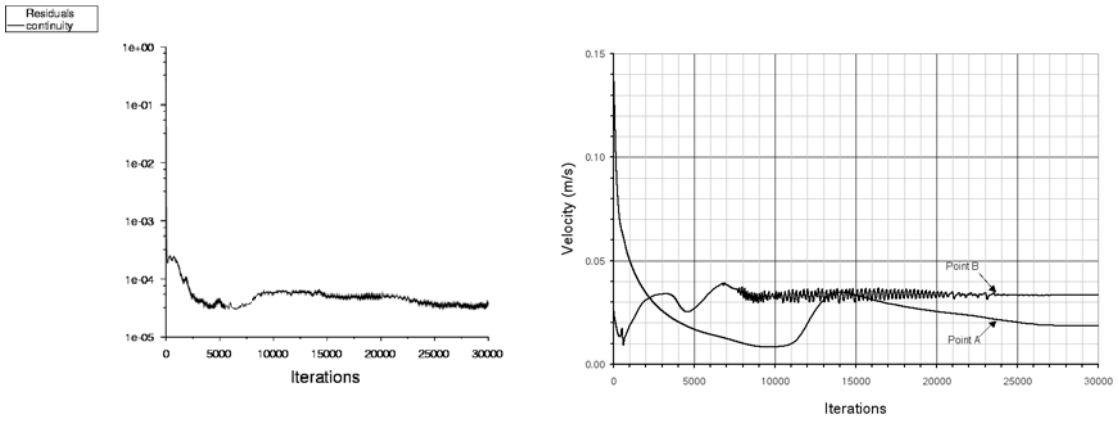

(a) Continuity Residual *(b) Points A and B*

Figure 2. *Convergence History*

5. GRID DEPENDENCY

To establish grid independent solutions three grids were evaluated. Grid A had 50x50x50 nodes along the *x, y, z* edges, respectively, of the walls and 10,000 nodes on the CSP surface resulting in a volume grid of 1.6×10^6 tetrahedral cells. The second, Grid B, was made up of 60x60x60 nodes along the *x, y, z* edges, respectively, of the walls and 20,000 nodes on the CSP surface resulting in a volume grid of 3.2×10^6 tetrahedral cells. A grid independent solution was established for the standard k-ε using Grids A and B but not so with the v^2-f. To reach grid convergence for the v^2-f, a third grid, Grid C, was needed. It was made up of 75x75x75 nodes along the *x, y, z* edges, respectively, of the walls and 42,000 nodes on the CSP surface.

For Grid C, twelve layers of prismatic boundary cells were extruded away from the CSP surface (Sørensen and Voigt 2003) to be able to resolve the viscous sub-layer and achieve the y^{+1} requirements of the v^2-f. The remaining volume was constructed with tetrahedral cells resulting in a hybrid grid of 4.5×10^6 total cells. By using only a tetrahedral topology it was difficult to create small near-wall cells while maintaining a good quality grid with a reasonable amount of cells. The average y^+ on the CSP for Grid B was 4.5 while the average y^+ for Grid C was 0.2 - over an order of magnitude smaller with an increase of only 50% more cells. Achieving a y^+ below 1 using only tetrahedral cells would have required tens of millions of cells.

To illustrate grid convergence, Fig. 3 shows a streamline starting from the same location in each of the three v^2-f solutions. It is clear that the streamline from Grid A is quite different than that from Grids B and C. In particular, the streamline in Grid A has circulated past the CSP a third time, becomes entrained in the thermal plume and exits the outlet. The streamline

---

[1] Where $y^+ = \frac{y_p u^*}{\nu}$: y_p is the distance from wall adjacent cell-center to the wall, the friction velocity $u^* = \sqrt{\frac{\tau_{wall}}{\rho}}$ and ν is the kinmatic viscosity

in Grids B and C only circulate past the CSP twice and finish forward and slightly to the left of the CSP. There are some small differences between the Grids B and C streamline but overall are very similar. All three solutions in Fig. 3 clearly show the recirculating flow structure caused by the inlet vent. For clarity, only single streamlines of equal lengths (500 sec.) were used for comparison. In contrast, the thermal plume predictions were found to be weakly dependent on the grid and more dependent on the turbulence model, discussed next (Sec. 6).

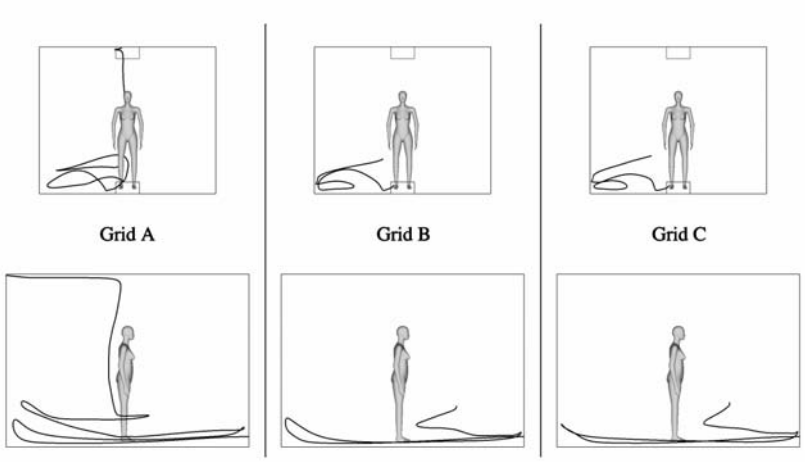

Figure 3. *Grid Dependency: v^2-f streamlines*

6. TURBULENCE MODELS

Modeling turbulence for personal micro-environment CFD simulations is challenging. Reynolds Averaged Navier-Stokes (RANS) models are popular because of their relative simplicity as well as requiring the lower computational resources. Their drawback is the lack of applicability to a wide range of problems. Typical RANS models assume the turbulence is locally isotropic. For the personal micro-environment this assumption may not always be correct, where natural convection is common and buoyancy generated turbulence is present (Hanjalić 2002, Tieszen et al. 1998). The personal micro-environment is also typified by low velocity flows where turbulence may be intermittent or not even present (i.e. transitional flow). Despite the many modifications made to the popular k-ε class of RANS models they may be inadequate for modeling these phenomena. A recent RANS model, the v^2-f of Durbin (1991), contains attributes that may help model these phenomena more accurately. In this work, the standard k-ε with an enhanced wall treatment along the third v^2-f variation of Sveningsson (2003), both available in FLUENT, were used.

The sensitivity of turbulence model on the thermal plume was obvious when standard k-ε and v^2-f results were compared (see Fig. 4). The thermal plume is much thicker around the CSP in the v^2-f solution. Also the magnitude of the velocity generated by the thermal plume was much higher for the v^2-f (0.35 *m/s*) as compared to the standard k-ε (0.20 *m/s*). While no experimental data was available for validation, Tieszen et al. (1998) had some success with the v^2-f for predictions of natural convection flows.

As with the grid study, large differences in the recirculating flow in room were observed between turbulence models. The consequence of this is that if one were interested in personal exposure then prediction of the room flow is as important as the thermal plume. Besides the mean velocity prediction, turbulence kinetic energy (TKE) plays an important role in PM transport. For PM transport in turbulent flows, a random fluctuating velocity is added to the mean velocity for the trajectory calculation. When using RANS models, the fluctuating

velocity is determined from the TKE by $\sqrt{\frac{2}{3}k} = \sqrt{u'^2} = \sqrt{v'^2} = \sqrt{w'^2}$. Figure 5 shows the difference in TKE predictions of the standard k-ε and v^2-f. While the standard k-ε predicted a higher maximum of TKE in the thermal plume above the CSP, the v^2-f predicted a more uniform distribution of TKE around the CSP. As well, the standard k-ε predicted more TKE in floor jet whereas the v^2-f almost none. A maximum TKE of around 0.0044 m^2/s^2 corresponds to a turbulence intensity of 27%. These levels of TKE emphasize the importance of turbulence prediction for PM transport.

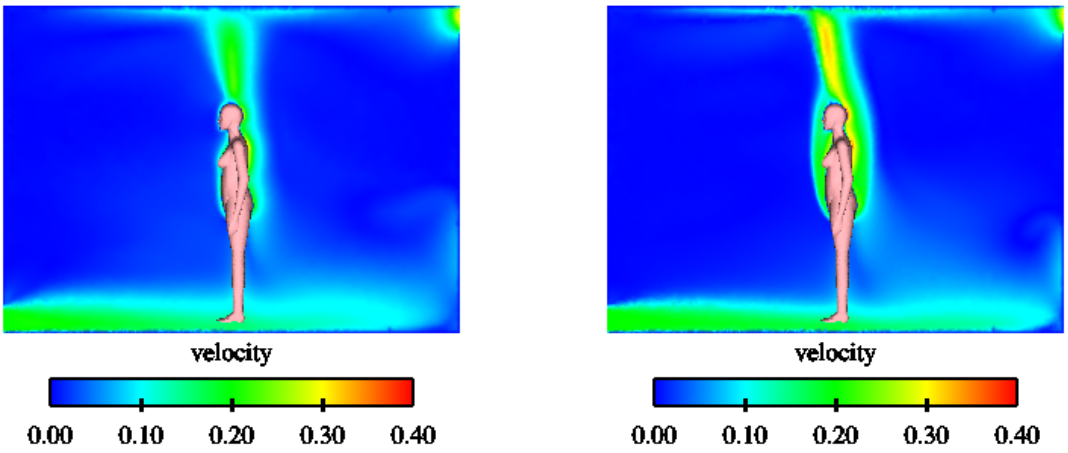

(a) standard k-ε (b) v^2-f

Figure 4. *Velocity Contours, x = 0.0 m*

7. CONCLUSIONS AND FUTURE CONSIDERATIONS

This study of the flow around a CSP in a displacement ventilated room examined the importance of convergence criteria, grid resolution and turbulence model. The level of detail used for the analyses was needed for a proper validation of CFD for the personal micro-environment.

To achieve complete convergence of the solution quantities other than average residual needed to be monitored. Because two distinct flow structures developed average residual was not a sufficient convergence parameter. Velocities were monitored at strategically chosen points during the iteration process. While the velocity in the thermal plume appeared to reach steady-state at approximately the same number of iterations as the residuals this was not so. At the point in the recirculating flow near the floor, the velocity oscillated for nearly 16,000 iterations before settling to a steady value. Over 26,000 iterations were needed to achieve convergence.

Grid independence was achieved for the standard k-ε on Grids A and B but the v^2-f required finer grid, Grid C. The v^2-f does not apply any ad-hoc functions, instead integrating the solution all the way through the boundary layer thus requiring a finer grid. Layers of thin prismatic cells were extruded from the CSP surface to resolve the boundary layer. While the thermal plume was found to be weakly dependent on the grid resolution, streamlines in the room were very different on Grid A than on Grids B and C for the v^2-f model.

Finally, two RANS turbulence models were compared. The standard k-ε solution differed considerably from the v^2-f solution. Comparison of the velocity contours showed the v^2-f predicted a thicker thermal plume and higher velocity than the standard k-ε. However, no experimental data was available for validation. Again, streamlines of the recirculating room

flow indicated differences between the models. Turbulence kinetic energy distribution and magnitude from each model were quite different throughout the entire solution. Together, accurate prediction of mean velocity (for flow path) and TKE (for fluctuating velocity) indicate the importance of turbulence model validation. This underscores the point that if one was interested in using CFD to study PM exposure, accurate prediction of the recirculating flow in the room is essential.

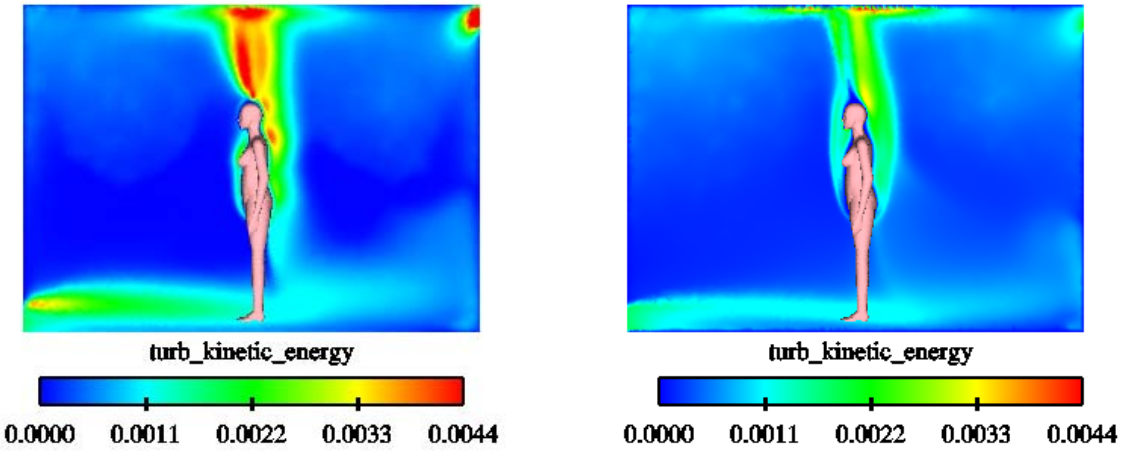

(a) standard k-ε (b) v^2-f

Figure 5. *Turbulence Kinetic Energy Contours, x = 0.0 m*

ACKNOWLEDGEMENTS

This work was supported by the US Environmental Protection Agency (EPA) through the STAR Center for Environmental Quality Systems (www.eqstar.org) and the Center of Excellence in Environmental Systems (www.coees.org) at Syracuse University.

REFERENCES

Nielsen, P.V., Murakami, S., Kato, S., Topp, C. Yang, J-H. 2003 "Benchmarks Test for a Computer Simulated Person", *Aalborg University, Indoor Environmental Engineering*

Durbin, P.A. 1991 "Near-Wall Turbulence Closure Modeling without 'Damping Functions'", *Theoretical and Computational Fluid Dynamics* Vol. 3, pp. 1-13

Hanjalić, K. 2002 "One-Point Closure Models for Buoyancy-Drive Turbulent Flows", *Annual Review of Fluid Mechanics* Vol. 43, pp. 321-347

Søresen, D.N. and Voigt L.K. 2003 "Modelling Flow and Heat Transfer around a Seated Human Body by Computational Fluid Dynamics", *Building and Environment* Vol. 38, pp. 753-762

Sveningsson, A. 2003 "Analysis of the Performance of Different v^2-f Turbulence Models in a Stator Vane Passage Flow", *PhD Thesis,* Chalmers University of Technology

Tieszen, S., Ooi, A., Durbin, P.A. and Behnia, M. 1998 "Modeling of Natural Convection Heat Transfer", *Proceedings of the Summer Program*, Center of Turbulence Research, Stanford University